J Biomol NMR (2013) 57:141–154
DOI 10.1007/s10858-013-9774-2

ARTICLE

Conformational stabilization of the membrane embedded targeting domain of the lysosomal peptide transporter TAPL for solution NMR

Franz Tumulka · Christian Roos · Frank Löhr · Christoph Bock · Frank Bernhard · Volker Dötsch · Rupert Abele

Received: 23 May 2013 / Accepted: 21 August 2013 / Published online: 7 September 2013

Abstract The ATP binding cassette transporter TAPL translocates cytosolic peptides into the lumen of lysosomes driven by the hydrolysis of ATP. Functionally, this transporter can be divided into coreTAPL, comprising the transport function, and an additional N-terminal transmembrane domain called TMD0, which is essential for lysosomal targeting and mediates the interaction with the lysosomal associated membrane proteins LAMP-1 and LAMP-2. To elucidate the structure of this unique domain, we developed protocols for the production of high quantities of cell-free expressed TMD0 by screening different N-terminal expression tags. Independently of the amino acid sequence, high expression was detected for AU-rich sequences in the first seven codons, decreasing the free energy of RNA secondary structure formation at translation initiation. Furthermore, avoiding NGG codons in the region of translation initiation demonstrated a positive effect on expression. For NMR studies, conditions were optimized for high solubilization efficiency, long-term stability, and high quality spectra. A most critical step was the careful exchange of the detergent used for solubilization by the detergent dihexanoylphosphatidylcholine. Several constructs of different size were tested in order to stabilize the fold of TMD0 as well as to reduce the conformation exchange. NMR spectra with sufficient resolution and homogeneity were finally obtained with a TMD0 derivative only modified by a C-terminal His_{10}-tag and containing a codon optimized AT-rich sequence.

Keywords ABC transporter · Peptide translocation · Cell-free expression · Translation initiation · N-terminal expression tag · Detergent exchange · Conformational stabilization

Abbreviations

β-OG	n-Octyl-β-D-glucopyranoside
Brij58	Polyethylene glycol hexadecyl ether
c7-DHPC	1,2-Diheptanoyl-*sn*-glycero-3-phosphocholine
DDM	n-Dodecyl-β-D-maltopyranoside
DHPC	1,2-Dihexanoyl-*sn*-glycero-3-phosphocholine
DPC	Dodecylphosphocholine
LDAO	n-Dodecyl-N,N-Dimethylamine-N-Oxide
LMPC	1-Myristoyl-2-hydroxy-*sn*-glycero-3-phosphocholine
LMPG	1-Myristoyl-2-hydroxy-*sn*-glycero-3-[phospho-rac-(1-glycerol)]
LPPG	1-Palmitoyl-2-hydroxy-*sn*-glycero-3-[phospho-rac-(1-glycerol)]
SDS	Sodium dodecyl sulfate
TROSY	Transverse relaxation optimized spectroscopy
TX100	Polyethylenglycol-mono-[*p*-(1,1,3,3-tetramethylbutyl)-phenyl]-ether

Introduction

The ATP binding cassette (ABC) transporter family is the largest class of primary transporters (Higgins 1992). ABC

Electronic supplementary material The online version of this article (doi:10.1007/s10858-013-9774-2) contains supplementary material, which is available to authorized users.

F. Tumulka · C. Bock · R. Abele (✉)
Institute of Biochemistry, Biocenter, Goethe-University Frankfurt, Max-von-Laue-Str. 9, 60438 Frankfurt am Main, Germany
e-mail: abele@em.uni-frankfurt.de

C. Roos · F. Löhr · F. Bernhard · V. Dötsch
Institute of Biophysical Chemistry, Biocenter, Goethe-University Frankfurt, Max-von-Laue-Str. 9, 60438 Frankfurt am Main, Germany

exporters are found in all organisms, whereas ABC importers are only present in prokaryots. In human, many diseases are connected to defective ABC transporters such as adenoleukodystrophy, diabetes mellitus, cystic fibrosis, and bare lymphocyte syndrome. Moreover, an increased expression of P-glycoprotein in tumor cells interferes with chemotherapy, due to arising multidrug resistance (Borst and Elferink 2002).

The transporter associated with antigen processing like (TAPL, ABCB9) is a lysosomal peptide transporter, translocating peptides from the cytosol into the lysosomal lumen driven by the hydrolysis of ATP (Zhang et al. 2000; Wolters et al. 2005; Demirel et al. 2007). TAPL has a broad peptide length specificity ranging from 6- to 59-mer peptides (Wolters et al. 2005). Peptide selectivity is restricted to the N-terminal and C-terminal positions (Zhao et al. 2008). Although the physiological function is not fully understood yet, the broad tissue distribution gives evidence that TAPL takes over a housekeeping function, clearing the cytosol from accumulating peptides (Zhang et al. 2000; Yamaguchi et al. 1999).

TAPL forms a homodimeric transport complex [Fig. 1, (Wolters et al. 2005; Leveson-Gower et al. 2004)]. Each subunit is composed of an N-terminal transmembrane domain (TMD) and a C-terminal nucleotide binding domain (NBD). In contrast to the general architecture of ABC exporters, containing 2×6 transmembrane helices, and based on sequence alignments and hydrophobicity analysis, the TMD of TAPL is composed of 2×10 transmembrane helices. Functionally, TAPL can be divided into the N-terminal transmembrane domain TMD0 (residues 1–142) and a core complex (Fig. 1). CoreTAPL is fully active in transport but is mistargeted to the plasma membrane (Demirel et al. 2010). TMD0 takes over a dual function in directing TAPL into lysosomes and mediating the interaction with the lysosome associated membrane proteins (LAMPs), thereby drastically increasing the half-life of this transporter (Demirel et al. 2010; Demirel et al. 2012). Although several molecular structures of ABC transporters are available, the structure of an additional transmembrane domain is not solved yet. Such a TMD0 is not only found in TAPL but also in the transporter associated with antigen processing (TAP) and in some members of the ABCC family. These extra membrane-embedded domains fulfill different functions like post-translational processing, intracellular trafficking, protein interaction, and activity regulation (Koch et al. 2004; Biemans-Oldehinkel et al. 2006; Chan et al. 2003; Bandler et al. 2008).

A prerequisite to close this structural gap is to produce high amounts of TMD0. Cell-free (CF) expression was found to be favourable for high membrane protein production since CF expression is not hampered by blockade of the protein secretion machinery and mRNA stability (Wagner et al. 2007; Reckel et al. 2010). Therefore, in *Escherichia coli* based CF expression protein yield mainly depends on translation efficiency, which strongly correlates with translation initiation. Stable secondary structures of the 5′ coding region of the mRNA severely reduces protein expression, whereas protein yield is dramatically increased if 5′ mRNA region displays a low tendency to form stable secondary structures (Kozak 2005). Therefore, N-terminal expression tags with a high AU content were developed with a low tendency to form stable 5′ mRNA structures as predicted by bioinformatics tools. A region of 42 nucleotides from −4 to +37 from the start codon was found to be critical for strong variation in expression of GFP variants (Kudla et al. 2009). However, as also sequences beyond this region influence protein yield, an empiric CF expression tag screening based on PCR templates could be an efficient alternative to computer based predictions (Haberstock et al. 2012).

Besides protein yield, the quality of the protein in terms of functionality and stability is critical for structural studies. Regarding membrane proteins, the screening for a favourable detergent is a crucial step since there is no dedicated prediction possible for choosing the proper detergent (Kim et al. 2009). Often, the detergent beneficial for solubilization is not appropriate for structural studies by solution NMR in respect to long-term stability and slow global motion of the protein because of the large micelle size or the presence of multiple conformations (Page et al. 2006). Therefore, a careful detergent exchange strategy has to be established (Arnold and Linke 2008).

Furthermore, the design of the construct has to be considered for structural studies. Disordered N- or C-terminal tags could contribute to multiple conformations, thus interfering with the determination of high resolution structures by NMR as well as by X-ray crystallography. Flexible tags may post-translationally be removed by specific proteolysis. However, sequence specific proteases can be strongly inhibited by detergent and remaining residues from the protease recognition site can still induce aggregation or conformational heterogeneity (Zanzoni et al. 2012). Although bioinformatics tools (Deng et al. 2012) and hydrogen/deuterium exchange mass spectrometry (Sharma et al. 2009) are used to identify disordered and unstructured regions in a protein, construct optimization for NMR is a tedious project with numerous trial and error attempts.

To solve the structure of the unique bifunctional, N-terminal transmembrane domain TMD0 of TAPL, we started a structural study by solution NMR. We describe the optimization of TMD0 production with a cell-free expression system and the sample improvement for solution NMR analysis by screening different detergents and template designs.

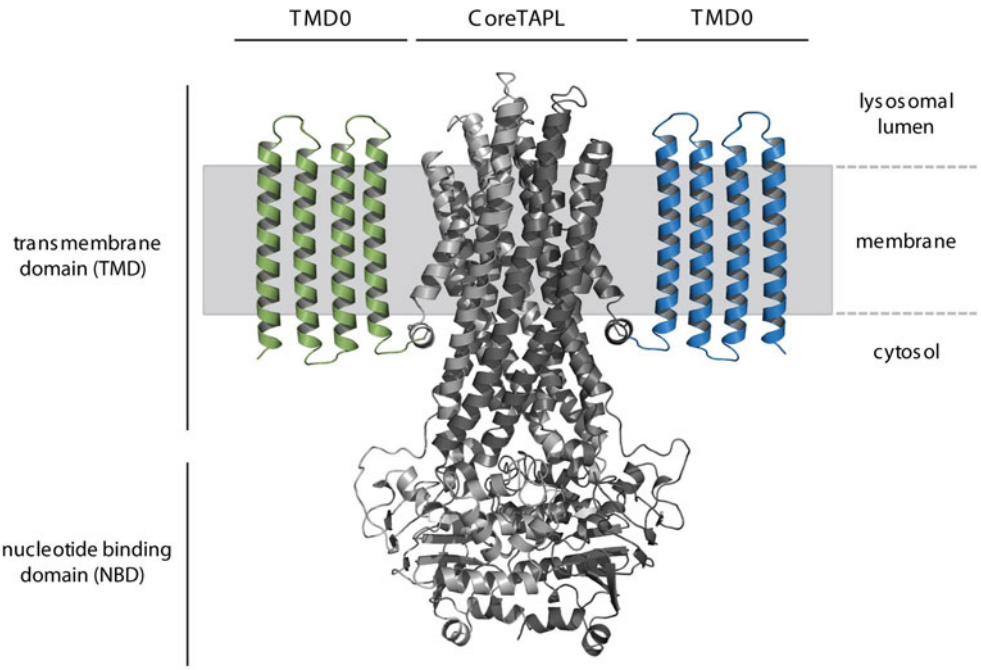

Fig. 1 Model of TAPL. Homodimeric coreTAPL (*light* and *dark grey*) was modelled on the X-ray structure of Sav1866 (PDB ID: 2ONJ). The N-terminal TMD0 (*green* and *blue*) is schematically depicted by four predicted helices connected by short loops

Experimental section

Cloning of TMD0 variants

As template, cysteine-less TMD0 (residue 1–142) of human TAPL (ABCB9, AAF89993.1) was used, in which all cysteines were replaced by alanines. TMD0 containing a N-terminal T7-tag and a C-terminal myc-tag followed by His_{10}-tag was generated by polymerase chain reaction using primers F1 and R1 and cloned into pET21a(+) vector (Merck, Darmstadt, Germany) via BamHI and XhoI restriction sites. For removal of the T7-tag, TMD0-myc-His_{10} was amplified with the primer pair F2 and R2 and recloned via NdeI and XhoI restriction sites into pET21a(+).

For tag variation, a pool of tag fragments consisting of the T7 promotor, ribosome binding site, tag of interest, and PreScission cleavage site sequence was generated with primer P1 and tag dependent primer P2 using pET21a(+) as template as described (Haberstock et al. 2012). The sequence of TMD0-myc-His_{10} in pET21a(+) was amplified by primer P3 and P4 including the T7 terminator. Subsequently, the polymerase chain reaction (PCR) products of the tag fragments and TMD0-myc-His_{10} were combined and amplified using primer P1 and P4 (Haberstock et al. 2012). PCR products of constructs containing a T7-tag or no tag at all were generated with primers P1 and P4 using the corresponding templates described above. The PCR products were directly used for expression screening.

TMD0 (residue 2–142) containing an N-terminal AU-rich expression tag followed by PreScission cleavage site and a C-terminal His_{10}-tag was generated using primers F3 and R3 and cloned into pIVex2.3-MCS vector (Roche, Mannheim, Germany) via NdeI and XhoI restriction sites. To shorten the construct for improved NMR spectra, the 5′ sequence of TMD0 was mutated to an AT-rich sequence by PCR with the primer pair F4 and R3 and cloned into pIVex2.3-MCS via NdeI and XhoI restriction sites. The free energy (ΔG) of secondary structures of the mRNAs was calculated using the DINAMelt server (http://mfold.rna.albany.edu/) starting from the first base of the mRNA to the seventh codon (Markham and Zuker 2005).

For site-directed spin labelling, serine at position 46 was replaced by QuickChange site directed mutagenesis (Qiagen, Hilden, Germany) using the primer pair F5 and R4 (Table 1).

Cell-free expression

CF expression was performed as described previously (Schneider et al. 2010; Schwarz et al. 2007). All analytical and preparative samples were expressed in the continuous exchange CF set-up. The reaction mix (RM) to feeding mix (FM) volumetric ratio was in the range of 1:15–1:17. RM volumes varied from 55 µl (analytical scale) to ≥1 ml (preparative scale). DNA templates were added in concentrations of 15–30 ng/µl to the RM. For optimal yields, the Mg^{2+} and K^{+} concentrations were adjusted for each construct and *E. coli* S30 extract preparation, ranging from 16 to 24 mM and 250 to 330 mM, respectively. The expression was carried out in the precipitation-CF (P-CF)

Table 1 Oligonucleotide primers

Primer	Orientation	Sequence
F1	Forward	5′-CGA TTA GGA TCC GAA TTC ATG CGG CTG TGG AAG GCG G-3′
R1	Reverse	5′-TAA TCG CTC GAG TCA GTG ATG GTG ATG GTG ATG GTG ATG GTG ATG GCA GCC CAG ATC CTC TTC TGA GAT GAG TTT TTG TTC ACT GCC TGG CCG CAC GGT GGA C-3′
F2	Forward	5′-CGA TTA CAT ATG CGG CTG TGG AAG GCG GTG G-3′
R2	Reverse	5′-GTG GTG GTG CTC GAG TCA GTG ATG GTG ATG-3′
P1	Forward	5′-GAT CGA GAT CTC GAT CCC GCG-3′
P4	Reverse	5′-GGA TAT AGT TCC TCC TTT CAG C-3′
P2 UCA	Reverse	5′-CGG GCC CTG AAA CAG CAC TTC CAG TGA TGA TGA TGA TGA TGA CAT ATG TAT ATC TCC TTC TTA-3′
P2 AU	Reverse	5′-CGG GCC CTG AAA CAG CAC TTC CAG ATA ATA TTT ATA ATA TTT CAT ATG TAT ATC TCC TTC TTA-3′
P2 GC	Reverse	5′-CGG GCC CTG AAA CAG CAC TTC CAG GCG CCG GCG CCG GCG CCG CAT ATG TAT ATC TCC TTC TTA-3′
P2 A-GC	Reverse	5′-CGG GCC CTG AAA CAG CAC TTC CAG GCG CCG GCG CCG GCG TTT CAT ATG TAT ATC TCC TTC TTA-3′
P3	Forward	5′-CTG GAA GTG CTG TTT CAG GGC CCG ATG CGG CTG TGG AAG GCG GTG GTG GTG-3′
F3	Forward	5′-GAT ATA CAT ATG AAA TAT TAT AAA TAT TAT CTG GAA GTG CTG TTT CAG GGC CCG CGG CTG TGG AAG GCG G-3′
R3	Reverse	5′-GTG GTG CTC GAG TCA TCA GTG ATG GTG ATG GTG ATG GTG ATG GTG ATG TGG CCG CAC GGT GGA CAG-3′
F4	Forward	5′-CGA TTA CAT ATG AAA TTA TAT AAA GCT GTT GTT GTT ACT TTG GCC TTC ATG AGT GTG GAC ATC-3′
F5	Forward	5′-CGC CAC TTC AAC ATC TTT GAC TGC GTG CTG GAT CTC-3′
R4	Reverse	5′-CTG CCC AGA GAT CCA GCA CGC AGT CAA AGA TGT TG-3′

Tag sequences are underlined

expression mode without adding detergents or lipids. Labeled amino acids were added for NMR samples (Cambridge Isotope Laboratories, Andover, MA, USA).

Protein solubilization and purification

The protein precipitate from the P-CF reaction was harvested by centrifugation at 21,000×*g* for 20 min at 4 °C. For pre-cleaning, the pellet was washed with one RM volume of H_2O followed by washing with one RM volume of TBS-I (20 mM Tris, 150 mM NaCl, 20 mM imidazole, pH 7.5). For NMR measurements without further purification or initial solubilization screens, the pellet was solubilized in 0.5 RM volumes of 25 mM Na-acetate pH 5.0 or TBS-I, respectively, supplemented with 1–3 % detergent for 2 h at room temperature and centrifuged for 20 min at 21,000×*g* and 4 °C. To visualize solubilization efficiency, the supernatant was separated by Tricine-SDS-PAGE (10 %) followed by immunoblotting using α-His-tag monoclonal antibody (Novagen, Schwalbach, Germany). For further purification, the pellet was incubated for 2 h at room temperature in one RM volume of TBS-I supplemented with 1 % detergent if not specified otherwise. Subsequently, the samples were centrifuged for 20 min at 21,000×*g* and 4 °C. The supernatant was incubated with Ni–NTA agarose (Qiagen) in a 6:1 volume ratio overnight at 4 °C. The Ni–NTA agarose was packed into a Poly-Prep chromatography column (Biorad, Munich, Germany) and washed with 10–50 column volumes of P-buffer (20 mM Tris, 500 mM NaCl, 20 mM imidazole, 1–2× critical micellar concentration (cmc) of detergent, pH 7.5). If DHPC was used for NMR spectroscopy, the initial detergent was exchanged on the Ni–NTA agarose column gradually by five washing steps W1–W5 (each step 10 column volumes; Table 2) with an increase of the DHPC concentration from 0.0 to 0.1 to 0.3 to 0.5 to 0.7 %. The protein was eluted with P-buffer containing 500 mM imidazole and 0.7 % DHPC. Afterwards, the buffer was exchanged on a PD-10 desalting column (GE Healthcare, Munich, Germany) to 25 mM Na-acetate pH 4.5–5.0, with or without 75 mM NaCl, 1× cmc detergent, and 1× HP protease inhibitor mix (Serva, Heidelberg, Germany). The protein was concentrated by an Amicon Ultra-2.0, 30 K concentrator (Merck Millipore, Schwalbach, Germany). Subsequently, the concentrated protein was centrifuged at 21,000×*g* for 20 min at 4 °C.

Table 2 Detergent concentration during washing steps (%)

	W1	W2	W3	W4	W5
LMPG	0.20	0.15	0.10	0.05	0.00
LPPG	0.15	0.10	0.05	0.03	0.00
SDS	0.50	0.30	0.20	0.10	0.00
LMPC	0.20	0.10	0.05	0.01	0.00

Site-directed spin labelling

For solubilization, purification, and detergent exchange to DHPC of single cysteine containing TMD0, 1 mM DTT was added to all buffers. After detergent exchange, protein bound on the Ni–NTA agarose column was washed with 10 column volumes of PD-buffer (P-buffer containing 0.7 % DHPC) to remove DTT. Afterwards, Ni–NTA agarose was incubated with 10 column volumes of PD-buffer containing 1.4 mM (1-oxyl-2,2,5,5-tetramethyl-Δ3-pyrroline-3-methyl) methanethiosulfonate (MTSL) for 1 h at 4 °C. Subsequently, column was washed by 10 column volumes of PD-buffer and protein was eluted with PD buffer containing 500 mM imidazole. Buffer exchange and concentration was performed as mentioned above.

Stability analysis

To evaluate the stability of TMD0, CF expressed protein was solubilized in 0.5 % LPPG and detergent was exchanged on the Ni–NTA column for the indicated detergent during a washing step of 10 column volumes. TMD0 was eluted with 20 mM Tris pH 7.5, 500 mM NaCl, 500 mM imidazole, 15 % glycerol supplemented with detergent. DHPC was exchanged as mentioned above. After incubation of TMD0 at 4 °C for up to 14 days or at different temperatures for 60 h, samples were centrifuged at 100,000×*g* for 45 min and supernatant was analyzed by Tricine-SDS-PAGE followed by Coomassie staining.

NMR spectroscopy

Experiments were recorded at static fields ranging from 600 to 950 MHz on Bruker Avance spectrometers equipped with cryogenic ^{1}H[^{13}C/^{15}N] triple-resonance probes. Two-dimensional ^{1}H-^{15}N correlations were obtained with a BEST-TROSY pulse sequence using a scan repetition time of 0.7 s (Favier and Brutscher 2011). Measurements were carried out at sample temperatures of either 40 or 50 °C. Acquisition times were 56 ms in the proton dimension and between 40 and 60 ms in the nitrogen dimension. Depending on protein concentrations, between 64 and 400 scans were accumulated per FID, giving rise to measurement times between approximately 4 and 24 h. Three-dimensional NOESY-[^{13}C,^{1}H]-HSQC and NOESY-[^{15}N,^{1}H]-TROSY experiments were carried out at 900 MHz using standard pulse sequences with mixing times of 60 ms. Each FID is the sum of eight transients corresponding to total measurement times of two and three days for ^{13}C- and ^{15}N-separated spectra, respectively.

Results

Cell-free expression protocol optimization

For structural investigation of TMD0 of human TAPL by NMR, we chose the *E. coli* based CF expression system since the expression of this membrane domain was toxic for *E. coli*. This CF expression benefits from high expression levels combined with reduced isotopic scrambling, thus allowing for amino acid type selective labeling schemes.

All CF expression studies were performed in the precipitation mode (P-CF), in which membrane proteins are synthesized in the absence of detergents or lipids and accumulate therefore in a precipitate. Often, these precipitated proteins can be successfully solubilized in their functional state by different detergents (Klammt et al. 2007a). The constructs tested contained different N-terminal expression tags for efficient translation initiation, followed by the sequence coding for PreScission cleavage to remove the N-terminal tag and the cysteine-less sequence of TMD0 (residue 2–142) coupled by a Gly-Ser linker with a myc-tag for immuno-detection. A Gly-Cys linker and a His_{10}-tag were added for labeling and purification at the C-terminus (Fig. 2, construct A). Since efficient translation initiation is crucial for high protein synthesis rates, we screened a set of short N-terminal expression tags comprising the first seven codons with a PCR based approach using linear DNA templates (Fig. 2

Fig. 2 Cell-free expressed constructs of TMD0. For expression tag screening, construct A (166-182 residues) composed of an N-terminal tag (*N-tag*; Table 3), a PreScission cleavage site (PreSc), *TMD0* (residue 2–142) coupled by a GlySer linker to a *myc*-tag and a His_{10}-tag was used. Purification, solubilization, and preliminary NMR spectra were established with construct B (166 residues). In construct C (152 residues), the beneficial AT-rich sequence was integrated into the 5′ region of *TMD0* by alternative codon usage and two mutations (R2K and W4Y)

Table 3 Codon usage and mRNA secondary structure stability

Construct/tag	Codon position at the 5′ end							ΔG^a range (kcal/mol)
	+1	+2	+3	+4	+5	+6	+7	
A/−	AUG	CGG	CUG	UGG	AAG	GCG	GUG	−22.2 to −21.1
	M	R	L	W	K	A	V	
A/T7	AUG	GCU	AGC	AUG	ACU	GGU	GGA	−21.0 to −20.1
	M	A	S	M	T	G	G	
A/UCA	AUG	UCA	UCA	UCA	UCA	UCA	UCA	−20.0 to −19.0
	M	S	S	S	S	S	S	
A/AU	AUG	AAA	UAU	UAU	AAA	UAU	UAU	−17.1 to −16.3
	M	K	Y	Y	K	Y	Y	
A/GC	AUG	CGG	CGC	CGG	CGC	CGG	CGC	−29.3 to −28.0
	M	R	R	R	R	R	R	
A/A-GC	AUG	AAA	CGC	CGG	CGC	CGG	CGC	−27.0 to −25.7
	M	K	R	R	R	R	R	
C/−	AUG	AAA	UUA	UAU	AAA	GCU	GUU	−16.7 to −15.7
	M	K	L	Y	K	A	V	

[a] Calculated for the 5′ region up to codon +7

and Table 3, constructs A) (Haberstock et al. 2012). The design of the tags were based on differences in secondary structure stability of the 5′ region of the mRNA and an AAA codon favorable at position +2. All tags had an AUG start codon. The T7 tag was demonstrated to be beneficial for CF expression of several G-protein coupled receptors (Klammt et al. 2007b). Since His-tags are often placed on the N-terminus, we tested an UCA-tag, which resembles the sequence of a His-tag with a frame shift of two bases, therefore coding for Ser_6 and thus stabilizing proteins according to the N-end rule in prokaryotes as well as in eukaryotes (Varshavsky 1997). The AU- and GC-tag are sequences only consisting of AU and GC bases with the lowest and highest energy of secondary structure stability of the 5′ region of the mRNA, respectively. In the A-GC-tag, an AAA codon substitutes a CGG codon of the GC-tag at position +2, since a triple A codon at this position is most frequently found in the genome of *E. coli*, enhancing protein expression.

The construct without any N-terminal-tag as well as the GC-tagged construct did not show any expression. The UCA-tagged, A-GC-tagged, and T7-tag containing constructs displayed weak expression (Fig. 3). The highest expression was detected for the construct comprising an N-terminal AU-tag, which shows the lowest stabilization of any secondary structures of the 5′ region of the mRNA as calculated by the DINAMelt server (http://mfold.rna.albany.edu/) (Table 3) (Markham and Zuker 2005). For further studies, we used a construct comprising the N-terminal AU-tag followed by a PreScission cleavage site, the cysteine-less TMD0, and a C-terminal His_{10} tag (Fig. 2, construct B). This optimized AU-tagged TMD0 construct showed a yield of up to 1 mg per 1 ml CF expression.

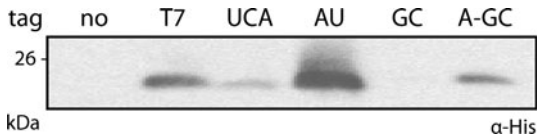

Fig. 3 Screening for N-terminal expression tags. PCR products of TMD0 containing different N-terminal sequences (Table 3) were used for CF expression of construct A. CF expression mix was separated by Tricine-SDS-PAGE (10 %) and TMD0 was detected by immunoblotting using α-His monoclonal antibody

Hydrophobic environment screening

After expression of membrane proteins in the P-CF mode, the precipitated protein has to be solubilized by detergent. To identify the optimal detergent, TMD0 solubilized in the presence of 1 % detergent (5 % for β-OG) was quantified (Fig. 4a). In addition to SDS, the phospholipid analogs DPC, LMPC, LMPG, and LPPG exhibited high solubilization efficiency. All other detergents tested were not suitable for the solubilization of TMD0. After solubilization, TMD0 was purified in a single step by Ni–NTA-agarose with a protein recovery of 80–100 % and a purity of more than 95 % (Fig. 4b). Structure determination by NMR spectroscopy requires the recording of spectra for hours and days. The correct folding and long-term stability of TMD0 in different detergents was therefore determined. To also include detergents which are not suitable for solubilization but are known to be favorable in stabilizing membrane proteins or to be beneficial for NMR, TMD0 was solubilized in LPPG and detergents were exchanged on the Ni–NTA column. All constructs of TMD0 showed a high α-helical content implying at least correct secondary structure formation (Fig. 1S). Moreover, TMD0 displayed

a high thermostability determined by CD spectroscopy in all detergents besides DDM (Fig. 1S). Concerning long-term stability, SDS and DPC but also Brij58 and DHPC stabilized TMD0 for 14 days at 4 °C, whereas TMD0 incubated in DDM as well as in LPPG or LMPG, which are very potent in solubilization, tended to aggregate over time (Fig. 4c). Brij58 is not suitable for NMR because of its large micelle size increasing the rotational correlation time of membrane proteins. SDS and DPC are very harsh detergents, known to unfold proteins. Therefore, we analyzed the thermostability of TMD0 for 60 h in the presence of DHPC at elevated temperatures which are suitable for liquid state NMR of detergent solubilized membrane proteins, showing rather long rotational correlation times leading to broad peaks and low sensitivity. These experiments demonstrated that no precipitation occurred up to 49 °C and that more than 50 % were still soluble after incubation at 60 °C (Fig. 4d).

Optimization of sample conditions

The experiments reported above have indicated that DHPC might be a good detergent for structural investigations. However, not all detergents that are good for protein stability are suitable for recording high resolution NMR spectra. Therefore, we solubilized TMD0 in LMPG, DPC, and SDS and recorded [^{15}N,^{1}H]-TROSY spectra without any purification step, since no other ^{15}N-labeled protein is present in the cell-free expression. All NMR studies were performed in 25 mM Na-acetate buffer pH 4.5–5.0, since TMD0 showed high stability in this buffer and amide proton exchange was slow. Detergent concentration varied from 1 to 3 %, due to different solubilization efficiencies. The spectra of TMD0 solubilized in LMPG, DPC, and SDS suffered from a low spectral resolution and, in some cases, showed signs of line broadening due to conformational exchange, suggesting that TMD0 does not form a stable tertiary structure under these conditions (Fig. 5a–c). As TMD0 displayed a high, long-term thermostability in DHPC and since it was demonstrated that DHPC is a favorable detergent for NMR studies on membrane proteins (Schnell and Chou 2008; Wang et al. 2009; Gautier et al. 2008), we solubilized TMD0 in LMPG, LPPG, LMPC, or SDS and exchanged the detergent on the Ni–NTA column gradually by DHPC. It is important that one of the two detergents lies above the critical micellar concentration. For the solubilization with phospholipid analogs, high yield of TMD0 was obtained after elution from the Ni–NTA column. Due to precipitation of TMD0 during detergent exchange from SDS, the recovery rate was only 25 % as compared to the other detergents. Independently from the detergent used for solubilization, the [^{15}N,^{1}H]-TROSY spectra in DHPC showed a better quality and wider ^{1}H

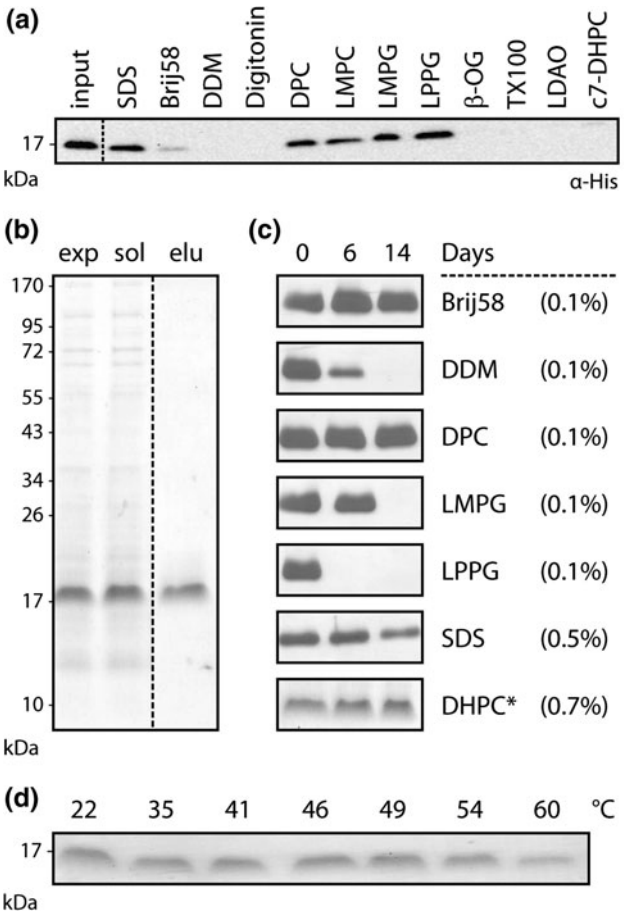

Fig. 4 Solubilization, purification, and long-term stability of TMD0. **a** Solubilization of TMD0. Solubilization efficiency of different detergents (1 % besides β-OG where 5 % were applied) for construct B was analyzed by Tricine-SDS-PAGE (10 %) followed by immunoblotting, using α-His monoclonal antibody. **b** Purification of TMD0. CF expressed construct B (exp) was solubilized by 1 % LMPG (sol) and purified by ion metal affinity chromatography (IMAC) (elu). Purity was analyzed by Tricine-SDS-PAGE (10 %) followed by Coomassie staining. **c** Long-term stability of TMD0. CF expressed construct A, solubilized in 0.5 % LPPG and exchanged by IMAC to detergent as indicated, was incubated at 4 °C up to 14 days in Tris buffer at pH 7.5 and soluble TMD0 was detected by SDS-PAGE (12 %) followed by Coomassie staining. For SDS, TMD0 was incubated at 22 °C. *Construct B was incubated in Na-acetate at pH 5.0. **d** Thermostability of TMD0. Construct C in DHPC was incubated for 60 h in Na-acetate pH 5.0 at different temperatures. Soluble TMD0 was identified by Tricine-SDS-PAGE (10 %) followed by Coomassie staining

chemical shift dispersion, which is a good indication for a folded protein (Fig. 5d, Fig. 2S). For all further studies, we used LMPG for solubilization followed by exchange to DHPC. To improve spectra quality, we optimized the DHPC and NaCl concentrations. The spectra of TMD0 in 1 and 2 % DHPC looked almost identical, whereas many peaks disappeared at higher concentrations of DHPC, presumably because of increased viscosity (Fig. 6). By testing different NaCl concentrations, the spectra of TMD0

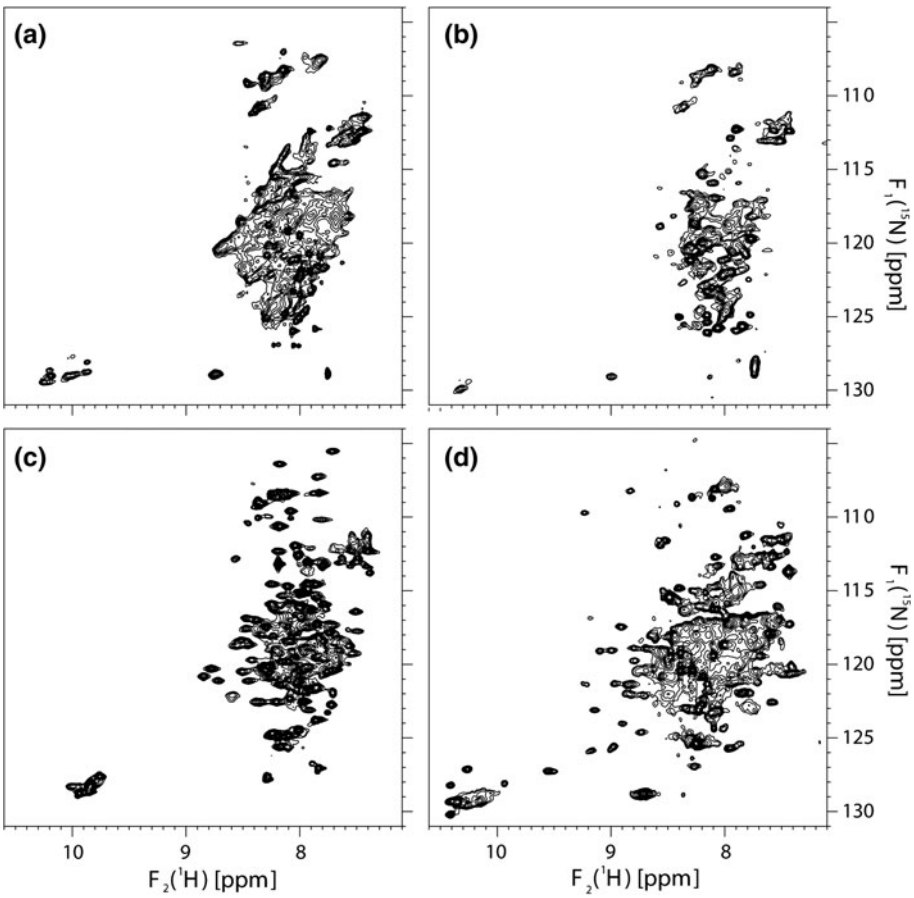

Fig. 5 Detergent dependent NMR spectra of TMD0. **a-c** TMD0 (construct B) was solubilized in 1 % LMPG (**a**, 100 μM TMD0), 3 % DPC (**b**, 100 μM TMD0) or 2 % SDS (**c**, 400 μM TMD0). **d.** TMD0 (construct B, 40 μM) was solubilized in 1 % LMPG and detergent was exchanged to 0.7 % DHPC. [^{15}N,^{1}H]-TROSY NMR spectra were recorded at 313 K in 25 mM Na-acetate pH 4.5–5.0

in the presence of 75 mM NaCl showed the highest quality with respect to signal intensity and chemical shift dispersion (Fig. 7a, b, Fig. 3S). After optimization of the spectra, we noticed that the number of peaks was higher than expected, suggesting that TMD0 exists in several conformations as derived from the tryptophan indole NH signals, where 15 peaks for 8 tryptophan residues are detected. This polydispersity was verified by TMD0 specifically labeled with ^{15}N isoleucine disclosing at least 20 signals for 9 isoleucine residues (Fig. 7a–c).

Stabilization of the TMD0 conformation

It is essential to get single signals per residue to resolve the structure of a protein by NMR. To stabilize a single conformation, we investigated larger constructs in which sequences C-terminal of TMD0 were attached, including one to three additional transmembrane helices of TAPL. Additionally, we joined to the N-terminus of TMD0 the transmembrane helix and the C-terminal, cytosolic part of LAMP-2B, which interacts with TAPL and stabilizes it. All these constructs were expressed and purified but the spectra were of low quality.

Since additional sequences did not lead to the stabilization of one single conformation of TMD0, we composed a construct of TMD0 missing any N-terminal tag extension. Since tag-less TMD0 was not expressed in the cell-free reaction, the codon usage of the first seven codons was adjusted to prevent stable mRNA secondary structures. Furthermore, NGG codons, known to decrease translation when located at the first five codons, were replaced by adenine and uracil rich codons coding for similar amino acids (R2K; W4Y) (Gonzalez de Valdivia and Isaksson 2004). As calculated by the DINAMelt server, the potential of the 5′ region of the mRNA to form secondary structures was drastically reduced from wt sequence ($\Delta G = -22.2$ to -21.1 kcal/mol) to this AU-rich sequence ($\Delta G = -16.7$ to -15.7 kcal/mol), which was even lower than the original AU-tag tested above ($\Delta G = -17.1$ to -16.3 kcal/mol) (Table 3). Taken together, the changes in the 5′ region of the mRNA resulted in the same expression yield of the tag-less TMD0 construct (from now on called construct C) as the AU-tagged construct B (Fig. 2).

Already in the absence of NaCl, the NMR spectrum of construct C showed a slightly improved quality. Although the number of peaks was reduced, one stable conformation was still not established as derived from the tryptophan side chain signals. By adding NaCl, the spectrum of tag-less TMD0 showed less overlap in the backbone region and indicated the existence of one single conformation based on the presence of seven signals for the

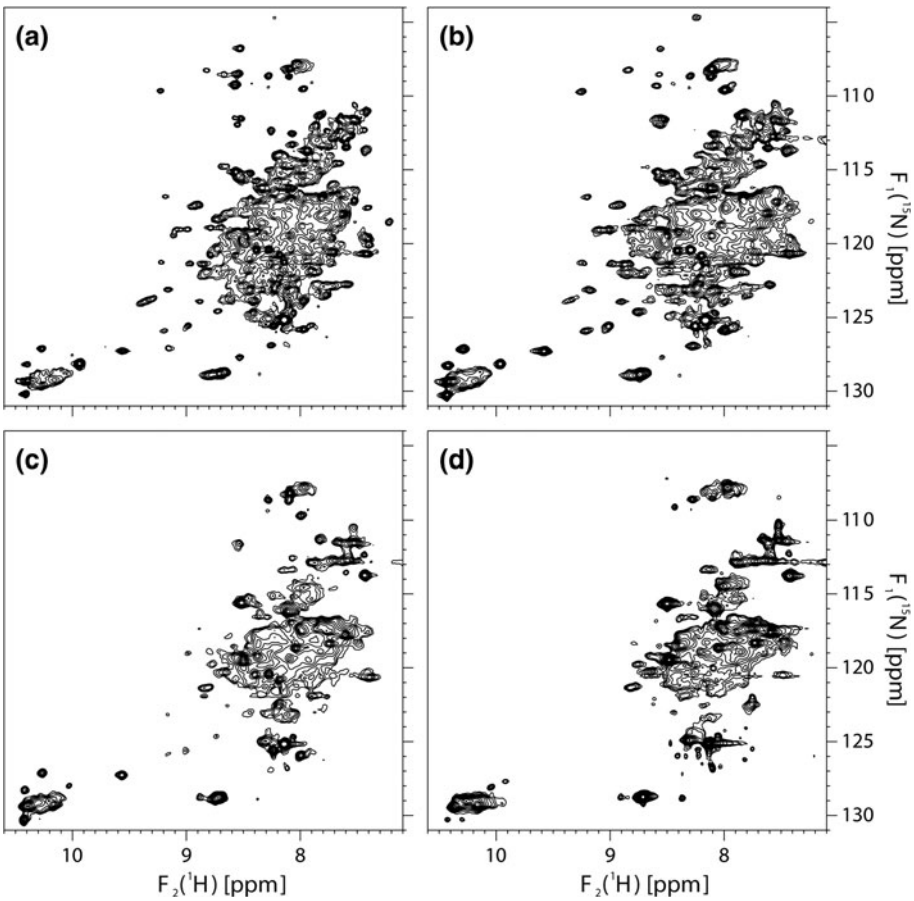

Fig. 6 DHPC concentration dependent NMR spectra. [^{15}N,^{1}H]-TROSY NMR spectra of TMD0 (Construct B; 130 μM) were recorded for 1 % (**a**), 2 % (**b**), 6 % (**c**), and 12 % (**d**) DHPC at 313 K in 25 mM Na-acetate pH 5.0

seven tryptophan side chains in construct C (Fig. 7d–f). The absence of conformational heterogeneity was validated by a [^{15}N,^{1}H]-TROSY spectrum of an ^{15}N isoleucine selectively labeled sample showing 10 peaks for the 9 isoleucines present in this construct with only one additional peak of low intensity at ~7.5 ppm (^{1}H) and ~116.5 ppm (^{15}N). This indicates a small amount of incorrectly folded protein present in the sample (Fig. 7f). Under these conditions, the rotational correlation of construct C was measured with a 2D version of the TRACT experiment (Lee et al. 2006), yielding a value of 25 ns at a temperature of 323 K.

Determination of spatial restraints

To substantiate the feasibility of structural studies of TMD0 using construct C initial NOESY data were obtained on a ^{13}C/^{15}N doubly labeled sample. Figure 8 shows representative proton–proton planes from ^{13}C- and ^{15}N-separated 3D NOESY spectra, both recorded with a mixing time of 60 ms. For a membrane protein, spectral quality and signal-to-noise ratio are reasonable and should enable the collection of a significant number of distance restraints. It is clear, however, that unambiguous assignment of NOEs will require collection of 4D ^{13}C, ^{13}C- and ^{15}N, ^{13}C-separated NOESY spectra and possibly the use of selectively labeled samples.

Since the number of long range NOEs obtained for α-helical membrane proteins is very limited, paramagnetic relaxation enhancement by paramagnetic spin labels is applied to receive additional valuable distance information in membrane proteins. Use of the nitroxide spin label MTSL requires engineering of single-cysteine mutants in which the cysteine side chains are accessible to the paramagnetic reagent with labelling efficiencies nearly 100 % but not too mobile. Figure 9 compares [^{15}N,^{1}H]-TROSY spectra of the S46C mutant of TMD0 with and without covalently attached MTSL. The absence of significant chemical shift changes compared to the cysteine-less protein (construct C) implies that the mutation does not give rise to structural distortions, a prerequisite for paramagnetic enhancement relaxation measurements. In the spin-labeled sample, a number of amide signals are not detected, indicating their proximity to the radical, while others have reduced intensity or are unaffected. It is expected that quantitative evaluation of such spectra from

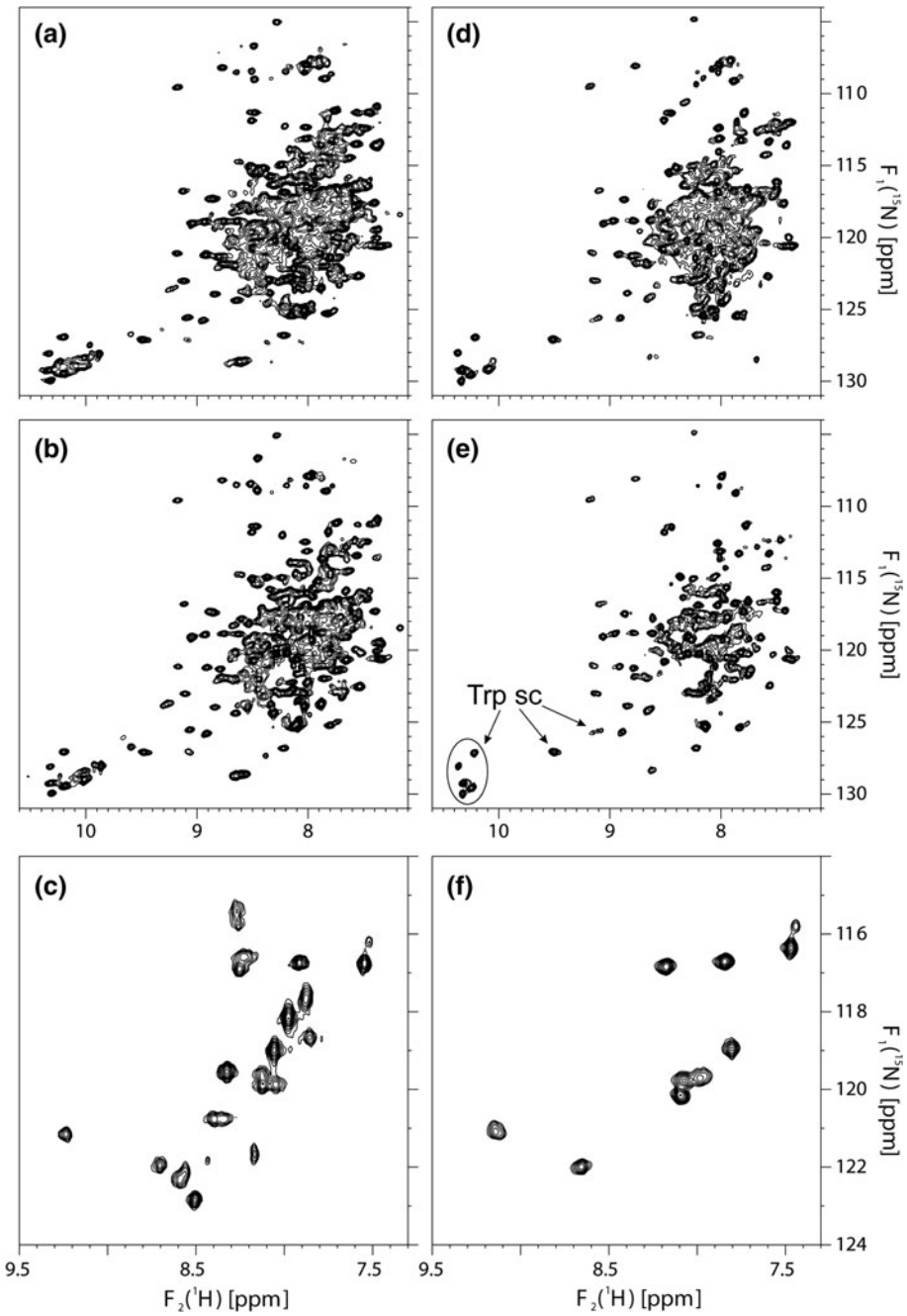

Fig. 7 Comparison of NMR spectra of construct B and C. [^{15}N,^{1}H]-TROSY NMR spectra of construct B (**a**–**c**) and C (**d**–**f**) in 1–2 % DHPC without (**a, d**) or with 75 mM NaCl (**b, c, e, f**) were recorded at 323 K in 25 mM Na-acetate pH 5.0. Conformational stability was investigated by ^{15}N Ile specific labelled TMD0 (**c, f**). **a, b** 100 μM TMD0, **c** 400 μM TMD0, **d-e** 25 μM TMD0 and **f** 140 μM TMD0. Signals from tryptophan side chains are depicted

this and other suitable mutants will provide upper and lower distance restraints for a structure determination of TMD0.

Discussion

This work aimed at optimizing the cell-free expression and sample conditions with respect to protein yield, quality, and stability suitable for high resolution NMR investigation of the targeting and interaction domain of the lysosomal peptide transporter TAPL. For structural studies by NMR, a high protein concentration (>400 μM) is needed to achieve a good signal-to-noise ratio. The best established system to fulfill all requirements is the expression in *E. coli* (Lundstrom et al. 2006; Tian et al. 2005; Wang et al. 2003). One disadvantage by using cell based expression is the inability to produce toxic proteins, as it was the case for TMD0 in our study. The *E. coli* based CF expression system is a perfect tool to overcome this problem, because it is independent of cellular integrity (Kim et al. 2009). Further advantages of this system are that many conditions can rapidly be screened

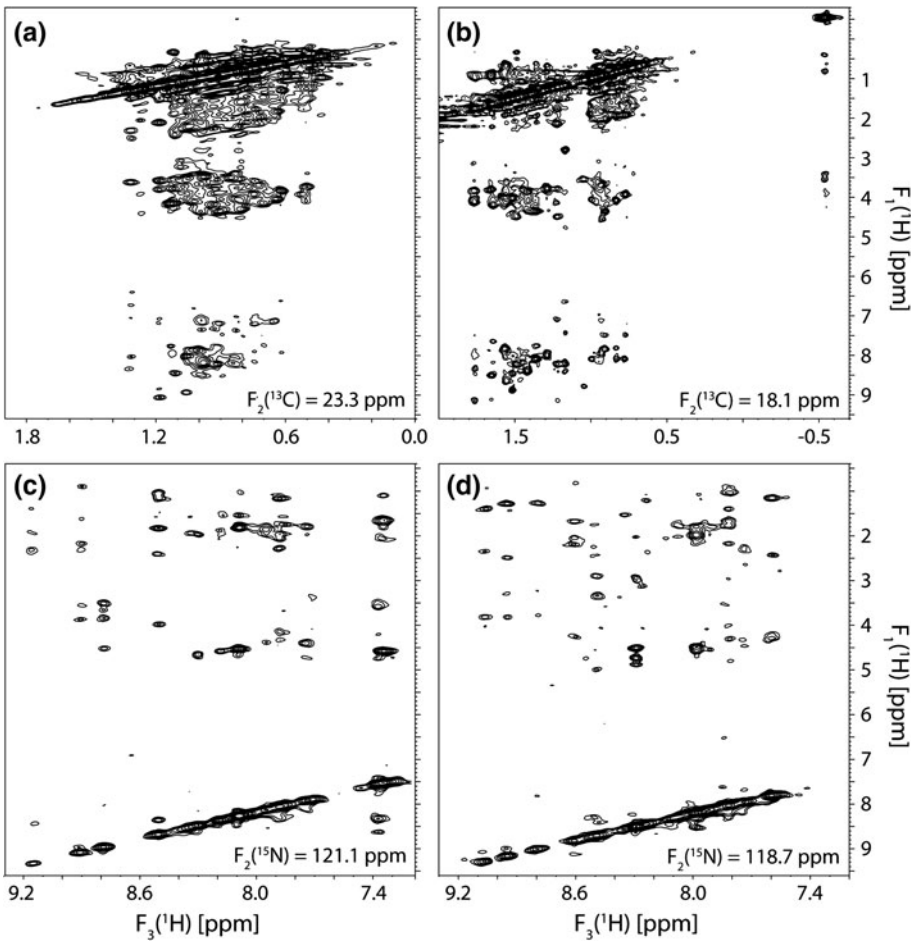

Fig. 8 [^{1}H]-NMR NOESY spectra. Depicted are [^{1}H,^{1}H]-planes of 3D NOESY-[^{13}C,^{1}H]-HSQC (**a, b**) and NOESY-[^{15}N,^{1}H]-TROSY (**c, d**) spectra (900 MHz) of [u-^{13}C;^{15}N]-labeled TMD0 (construct C, 600 μM) in 2 % DHPC recorded at 323 K. Heteronuclear chemical shifts at which the slices are extracted are indicated in the lower right corner of each panel

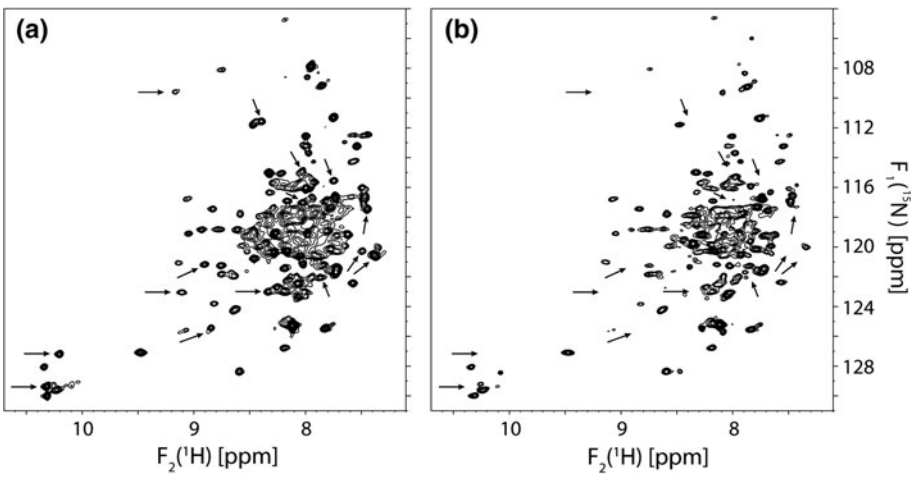

Fig. 9 Paramagnetic relaxation enhancement. [^{15}N,^{1}H]-TROSY NMR spectra (800 MHz) of the single cysteine mutant S46C of TMD0 (200 μM) in the absence (**a**) and presence (**b**) of covalently bound, oxidized MTSL were recorded at 323 K. The position of some resolved signal broadened beyond detection in the paramagnetic state is indicated by *arrows*

(Klammt et al. 2012), isotope labeled proteins can be measured by NMR without any labor intensive purification steps and amino acid type selective labeling schemes are possible due to strongly reduced isotopic scrambling (Kainosho et al. 2006; Klammt et al. 2004; Löhr et al. 2012).

The need for high protein concentrations requires an elevated expression yield. As reported by Haberstock et al., additions in the N-terminal region can enhance protein production by up to 30-fold (Haberstock et al. 2012). One aspect that lowers protein expression regards stable mRNA secondary structures, previously shown for GFP with different N-terminal extensions (Goltermann et al. 2011). Accordingly, the AU-tag with the lowest stabilization of mRNA secondary structures ($\Delta G = -17.1$ to -16.3 kcal/mol)

showed the highest expression of TMD0 and the GC-tag with the most stable mRNA secondary structures ($\Delta G = -29.3$ to -28.0 kcal/mol) gave no expression at all (Fig. 3, Table 3). However, this is not the only criterion, since one codon exchange from CGG to AAA at position +2 (A-GC-tag) resulted in a detectable expression, although there is a strong secondary structure formation ($\Delta G = -27.0$ to -25.7 kcal/mol). This was in agreement with former studies, which revealed that the second codon position is crucial for expression rates (Ahn et al. 2007). This single codon exchange presented higher expression yields than the tag-less and UCA-tagged TMD0, although they exhibit more favorable ΔG values of -22.2 to -21.1 kcal/mol and -20.0 to -19.0 kcal/mol, respectively. Especially the NGG motif at the first five codon positions is known to result in poor protein amounts, as investigated for lacZ expression in *E.coli* (Gonzalez de Valdivia and Isaksson 2004). The strategy of lowering the mRNA secondary structure stability and the avoidance of suboptimal codon compositions were then used for the construction of a tag-less TMD0 with similar N-terminal properties as the WT protein. The optimized construct showed the same expression yield as the AU-tagged version with the benefit of no added sequences at the N-terminus, which can influence the temperature stability of proteins as reported for staphylococcal lipases with an N-terminal His-tag (Sayari et al. 2007) or which could cause conformational heterogeneity as in the case of TMD0.

Although it is possible to carry out NMR measurements immediately after solubilization of the protein precipitate from the expression mixture, in our hands we could not obtain correctly folded protein although secondary structure elements were formed. All three detergents used gave poor spectrum qualities, even though they were suitable for other proteins (Klammt et al. 2012; Hwang et al. 2002; Zhou et al. 2008; Baker et al. 2007; Van Horn et al. 2009). Therefore, it seems that TMD0 forms a molten globule during cell free expression in the precipitation mode and the strong detergents tested cannot induce tertiary structure formation. After purification and detergent exchange to DHPC, the dispersion of the spectrum was much broader, reflecting a protein with a stable tertiary structure. Hereby, the detergent used for solubilization had no impact on the spectrum quality. Since it has been shown that the detergent concentration can influence the spectrum (Nietlispach and Gautier 2011), we tested concentrations up to 12 % of DHPC. Too high detergent amounts led to an increased viscosity and the disappearing of many peaks. Adding NaCl had a positive effect, resulting in the stabilization of a single conformation of TMD0. Salt concentrations higher than 100 mM, however, led to a reduced sensitivity.

The α-helices of the predicted four helix bundle show a very high thermostability since the CD signal at 222 nm did not change significantly for mild detergents like DHPC but also harsh ones like SDS during heating. The change of the CD signal in the presence of DDM above 50 °C and c7-DHPC above 80 °C resulted from precipitation. The collapse of tertiary structure at higher temperature cannot be determined since the far-UV signal only reflects the amount of secondary structure. Melting of tertiary structure without changes in secondary structure is reported for example for lysozyme or the glycerol facilitator in detergent solution (Knubovets et al. 1999; Galka et al. 2008).

The results reported here demonstrate that the quality of NMR spectra of membrane proteins can be drastically improved by optimizing solubilization of P-CF generated samples by systematically screening (1) the detergent type and concentration used for recording the NMR spectra, (2) buffer conditions as well as (3) the design of the expression construct. Based on this optimization procedure, it will now be possible to determine the solution NMR structure of TMD0 solubilized in DHPC.

Conclusion

There exists an increasing number of high resolution structures of ABC transporters. The structure of the core of ABC exporters, composed of 2 × 6 transmembrane helices and two nucleotide binding domains, is very similar. Nevertheless, there also are additional soluble as well as membrane-embedded domains involved in correct folding, substrate specificity, transporter dimerization, transport activity, subcellular localization, and interaction with cellular factors (Biemans-Oldehinkel et al. 2006). For the lysosomal peptide transporter TAPL, the N-terminal membrane-embedded domain TMD0 has a dual function by mediating the subcellular targeting as well as the interaction with the lysosomal associated membrane proteins LAMP-1 and LAMP-2, which strongly stabilize TAPL. In the course of this study, we optimized the CF expression of TMD0 by screening N-terminal expression tags. It became obvious that an AU-rich sequence in the translation initiation region enhances expression as reported previously (Goltermann et al. 2011). Nonetheless, this additional tag induced a conformational instability. Avoiding the N-terminal extension and simultaneously mutating the 5′ codons of the mRNA to an AU-rich sequence resulted in a single stable conformation of TMD0 suitable for structural investigation by NMR. This will bring us a step forward in the understanding of ABC transporters. In summary, the starting point for structural investigation is to find optimal conditions for a long-term stable protein in a single conformation. In this respect, expression conditions including expression source and translation initiation sequence, purification, ionic strength,

concentration, and type of detergent in case of membrane proteins as well as N- and C-terminal extensions of the construct have to be considered.

Acknowledgments We thank Christine Le Gal for preparing the manuscript. This work is supported by German Research Foundation (SFB 807—F.T., C.R., F.B., V.D., R.A.), NIH (U54 GM094608), the Center for Biomolecular Magnetic Resonance (BMRZ) and the Cluster of Excellence Frankfurt (Macromolecular Complexes).

References

Ahn JH, Hwang MY, Lee KH, Choi CY, Kim DM (2007) Use of signal sequences as an in situ removable sequence element to stimulate protein synthesis in cell-free extracts. Nucleic Acids Res 35(4):e21. doi:10.1093/nar/gkl917

Arnold T, Linke D (2008) The use of detergents to purify membrane proteins. Curr Protoc Protein Sci Chapter 4: Unit 4.8.1-4.8.30. doi:10.1002/0471140864.ps0408s53

Baker KA, Tzitzilonis C, Kwiatkowski W, Choe S, Riek R (2007) Conformational dynamics of the KcsA potassium channel governs gating properties. Nat Struct Mol Biol 14(11):1089–1095. doi:10.1038/nsmb1311

Bandler PE, Westlake CJ, Grant CE, Cole SP, Deeley RG (2008) Identification of regions required for apical membrane localization of human multidrug resistance protein 2. Mol Pharmacol 74(1):9–19. doi:10.1124/mol.108.045674

Biemans-Oldehinkel E, Doeven MK, Poolman B (2006) ABC transporter architecture and regulatory roles of accessory domains. FEBS Lett 580(4):1023–1035. doi:10.1016/j.febslet.2005.11.079

Borst P, Elferink RO (2002) Mammalian ABC transporters in health and disease. Annu Rev Biochem 71:537–592. doi:10.1146/annurev.biochem.71.102301.093055

Chan KW, Zhang H, Logothetis DE (2003) N-terminal transmembrane domain of the SUR controls trafficking and gating of Kir6 channel subunits. EMBO J 22(15):3833–3843. doi:10.1093/emboj/cdg376

Demirel O, Waibler Z, Kalinke U, Grunebach F, Appel S, Brossart P, Hasilik A, Tampé R, Abele R (2007) Identification of a lysosomal peptide transport system induced during dendritic cell development. J Biol Chem 282(52):37836–37843. doi:10.1074/jbc.M708139200

Demirel O, Bangert I, Tampé R, Abele R (2010) Tuning the cellular trafficking of the lysosomal peptide transporter TAPL by its N-terminal domain. Traffic 11(3):383–393. doi:10.1111/j.1600-0854.2009.01021.x

Demirel O, Jan I, Wolters D, Blanz J, Saftig P, Tampé R, Abele R (2012) The lysosomal polypeptide transporter TAPL is stabilized by interaction with LAMP-1 and LAMP-2. J Cell Sci 125(Pt 18):4230–4240. doi:10.1242/jcs.087346

Deng X, Eickholt J, Cheng J (2012) A comprehensive overview of computational protein disorder prediction methods. Mol BioSyst 8(1):114–121. doi:10.1039/c1mb05207a

Favier A, Brutscher B (2011) Recovering lost magnetization: polarization enhancement in biomolecular NMR. J Biomol NMR 49(1):9–15. doi:10.1007/s10858-010-9461-5

Galka JJ, Baturin SJ, Manley DM, Kehler AJ, O'Neil JD (2008) Stability of the glycerol facilitator in detergent solutions. Biochemistry 47(11):3513–3524. doi:10.1021/bi7021409

Gautier A, Kirkpatrick JP, Nietlispach D (2008) Solution-state NMR spectroscopy of a seven-helix transmembrane protein receptor: backbone assignment, secondary structure, and dynamics. Angew Chem Int Ed Engl 47(38):7297–7300. doi:10.1002/anie.200802783

Goltermann L, Borch Jensen M, Bentin T (2011) Tuning protein expression using synonymous codon libraries targeted to the 5′ mRNA coding region. Protein Eng Des Sel 24(1–2):123–129. doi:10.1093/protein/gzq086

Gonzalez de Valdivia EI, Isaksson LA (2004) A codon window in mRNA downstream of the initiation codon where NGG codons give strongly reduced gene expression in Escherichia coli. Nucleic Acids Res 32(17):5198–5205. doi:10.1093/nar/gkh857

Haberstock S, Roos C, Hoevels Y, Dötsch V, Schnapp G, Pautsch A, Bernhard F (2012) A systematic approach to increase the efficiency of membrane protein production in cell-free expression systems. Protein Expr Purif 82(2):308–316. doi:10.1016/j.pep.2012.01.018

Higgins CF (1992) ABC transporters: from microorganisms to man. Annu Rev Cell Biol 8:67–113. doi:10.1146/annurev.cb.08.110192.000435

Hwang PM, Choy WY, Lo EI, Chen L, Forman-Kay JD, Raetz CR, Prive GG, Bishop RE, Kay LE (2002) Solution structure and dynamics of the outer membrane enzyme PagP by NMR. Proc Natl Acad Sci USA 99(21):13560–13565. doi:10.1073/pnas.212344499

Kainosho M, Torizawa T, Iwashita Y, Terauchi T, Mei Ono A, Guntert P (2006) Optimal isotope labelling for NMR protein structure determinations. Nature 440(7080):52–57. doi:10.1038/nature04525

Kim HJ, Howell SC, Van Horn WD, Jeon YH, Sanders CR (2009) Recent advances in the application of solution NMR Spectroscopy to multi-span integral membrane proteins. Prog Nucl Magn Reson Spectrosc 55(4):335–360. doi:10.1016/j.pnmrs.2009.07.002

Klammt C, Löhr F, Schäfer B, Haase W, Dötsch V, Ruterjans H, Glaubitz C, Bernhard F (2004) High level cell-free expression and specific labeling of integral membrane proteins. Eur J Biochem 271(3):568–580

Klammt C, Schwarz D, Dötsch V, Bernhard F (2007a) Cell-free production of integral membrane proteins on a preparative scale. Methods Mol Biol 375:57–78. doi:10.1007/978-1-59745-388-2_3

Klammt C, Schwarz D, Eifler N, Engel A, Piehler J, Haase W, Hahn S, Dötsch V, Bernhard F (2007b) Cell-free production of G protein-coupled receptors for functional and structural studies. J Struct Biol 158(3):482–493. doi:10.1016/j.jsb.2007.01.006

Klammt C, Maslennikov I, Bayrhuber M, Eichmann C, Vajpai N, Chiu EJ, Blain KY, Esquivies L, Kwon JH, Balana B, Pieper U, Sali A, Slesinger PA, Kwiatkowski W, Riek R, Choe S (2012) Facile backbone structure determination of human membrane proteins by NMR spectroscopy. Nat Methods 9(8):834–839. doi:10.1038/nmeth.2033

Knubovets T, Osterhout JJ, Connolly PJ, Klibanov AM (1999) Structure, thermostability, and conformational flexibility of hen egg-white lysozyme dissolved in glycerol. Proc Natl Acad Sci USA 96(4):1262–1267

Koch J, Guntrum R, Heintke S, Kyritsis C, Tampé R (2004) Functional dissection of the transmembrane domains of the transporter associated with antigen processing (TAP). J Biol Chem 279(11):10142–10147. doi:10.1074/jbc.M312816200

Kozak M (2005) Regulation of translation via mRNA structure in prokaryotes and eukaryotes. Gene 361:13–37. doi:10.1016/j.gene.2005.06.037

Kudla G, Murray AW, Tollervey D, Plotkin JB (2009) Coding-sequence determinants of gene expression in Escherichia coli. Science 324(5924):255–258. doi:10.1126/science.1170160

Lee D, Hilty C, Wider G, Wuthrich K (2006) Effective rotational correlation times of proteins from NMR relaxation interference. J Magn Reson 178(1):72–76. doi:10.1016/j.jmr.2005.08.014

Leveson-Gower DB, Michnick SW, Ling V (2004) Detection of TAP family dimerizations by an in vivo assay in mammalian cells. Biochemistry 43(44):14257–14264. doi:10.1021/bi049124 5

Löhr F, Reckel S, Karbyshev M, Connolly PJ, Abdul-Manan N, Bernhard F, Moore JM, Dötsch V (2012) Combinatorial triple-selective labeling as a tool to assist membrane protein backbone resonance assignment. J Biomol NMR 52(3):197–210. doi:10.1007/s10858-012-9601-1

Lundstrom K, Wagner R, Reinhart C, Desmyter A, Cherouati N, Magnin T, Zeder-Lutz G, Courtot M, Prual C, Andre N, Hassaine G, Michel H, Cambillau C, Pattus F (2006) Structural genomics on membrane proteins: comparison of more than 100 GPCRs in 3 expression systems. J Struct Funct Genomics 7(2):77–91. doi:10.1007/s10969-006-9011-2

Markham NR, Zuker M (2005) DINAMelt web server for nucleic acid melting prediction. Nucleic Acids Res 33 (Web Server issue):W577–W581. doi:10.1093/nar/gki591

Nietlispach D, Gautier A (2011) Solution NMR studies of polytopic alpha-helical membrane proteins. Curr Opin Struct Biol 21(4):497–508. doi:10.1016/j.sbi.2011.06.009

Page RC, Moore JD, Nguyen HB, Sharma M, Chase R, Gao FP, Mobley CK, Sanders CR, Ma L, Sonnichsen FD, Lee S, Howell SC, Opella SJ, Cross TA (2006) Comprehensive evaluation of solution nuclear magnetic resonance spectroscopy sample preparation for helical integral membrane proteins. J Struct Funct Genomics 7(1):51–64. doi:10.1007/s10969-006-9009-9

Reckel S, Sobhanifar S, Durst F, Lohr F, Shirokov VA, Dotsch V, Bernhard F (2010) Strategies for the cell-free expression of membrane proteins. Methods Mol Biol 607:187–212. doi:10.1007/978-1-60327-331-2_16

Sayari A, Mosbah H, Verger R, Gargouri Y (2007) The N-terminal His-tag affects the enantioselectivity of staphylococcal lipases: a monolayer study. J Colloid Interface Sci 313(1):261–267. doi:10.1016/j.jcis.2007.04.053

Schneider B, Junge F, Shirokov VA, Durst F, Schwarz D, Dötsch V, Bernhard F (2010) Membrane protein expression in cell-free systems. Methods Mol Biol 601:165–186. doi:10.1007/978-1-60761-344-2_11

Schnell JR, Chou JJ (2008) Structure and mechanism of the M2 proton channel of influenza A virus. Nature 451(7178):591–595. doi:10.1038/nature06531

Schwarz D, Junge F, Durst F, Frolich N, Schneider B, Reckel S, Sobhanifar S, Dötsch V, Bernhard F (2007) Preparative scale expression of membrane proteins in Escherichia coli-based continuous exchange cell-free systems. Nat Protoc 2(11):2945–2957. doi:10.1038/nprot.2007.426

Sharma S, Zheng H, Huang YJ, Ertekin A, Hamuro Y, Rossi P, Tejero R, Acton TB, Xiao R, Jiang M, Zhao L, Ma LC, Swapna GV, Aramini JM, Montelione GT (2009) Construct optimization for protein NMR structure analysis using amide hydrogen/deuterium exchange mass spectrometry. Proteins 76(4):882–894. doi:10.1002/prot.22394

Tian C, Karra MD, Ellis CD, Jacob J, Oxenoid K, Sonnichsen F, Sanders CR (2005) Membrane protein preparation for TROSY NMR screening. Methods Enzymol 394:321–334. doi:10.1016/S0076-6879(05)94012-3

Van Horn WD, Kim HJ, Ellis CD, Hadziselimovic A, Sulistijo ES, Karra MD, Tian C, Sonnichsen FD, Sanders CR (2009) Solution nuclear magnetic resonance structure of membrane-integral diacylglycerol kinase. Science 324(5935):1726–1729. doi:10.1126/science.1171716

Varshavsky A (1997) The N-end rule pathway of protein degradation. Genes Cells 2(1):13–28

Wagner S, Baarst L, Ytterberg AJ, Klussmeier A, Wagner CS, Nord O, Nygren PA, van Wijk KJ, de Gier JW (2007) Consequences of membrane protein overexpression in Escherichia coli. Mol Cell Proteomics 6(9):1527–1550. doi:10.1074/mcp.M600431-MCP200

Wang DN, Safferling M, Lemieux MJ, Griffith H, Chen Y, Li XD (2003) Practical aspects of overexpressing bacterial secondary membrane transporters for structural studies. Biochim Biophys Acta 1610(1):23–36

Wang J, Pielak RM, McClintock MA, Chou JJ (2009) Solution structure and functional analysis of the influenza B proton channel. Nat Struct Mol Biol 16(12):1267–1271. doi:10.1038/nsmb.1707

Wolters JC, Abele R, Tampé R (2005) Selective and ATP-dependent translocation of peptides by the homodimeric ATP binding cassette transporter TAP-like (ABCB9). J Biol Chem 280(25):23631–23636. doi:10.1074/jbc.M503231200

Yamaguchi Y, Kasano M, Terada T, Sato R, Maeda M (1999) An ABC transporter homologous to TAP proteins. FEBS Lett 457(2):231–236

Zanzoni S, D'Onofrio M, Molinari H, Assfalg M (2012) Recombinant proteins incorporating short non-native extensions may display increased aggregation propensity as detected by high resolution NMR spectroscopy. Biochem Biophys Res Commun 427(3):677–681. doi:10.1016/j.bbrc.2012.09.121

Zhang F, Zhang W, Liu L, Fisher CL, Hui D, Childs S, Dorovini-Zis K, Ling V (2000) Characterization of ABCB9, an ATP binding cassette protein associated with lysosomes. J Biol Chem 275(30):23287–23294. doi:10.1074/jbc.M001819200

Zhao C, Haase W, Tampé R, Abele R (2008) Peptide specificity and lipid activation of the lysosomal transport complex ABCB9 (TAPL). J Biol Chem 283(25):17083–17091. doi:10.1074/jbc.M801794200

Zhou Y, Cierpicki T, Jimenez RH, Lukasik SM, Ellena JF, Cafiso DS, Kadokura H, Beckwith J, Bushweller JH (2008) NMR solution structure of the integral membrane enzyme DsbB: functional insights into DsbB-catalyzed disulfide bond formation. Mol Cell 31(6):896–908. doi:10.1016/j.molcel.2008.08.028